Progress In Electromagnetics Research C, Vol. 104, 201–214, 2020

A Switchable Triple-Band Notched UWB Antenna Using Compact Multi-Via Electromagnetic Band Gap Structure

Vijay R. Kapure[1, *], Pramod P. Bhavarthe[2], and Surendra S. Rathod[3]

Abstract—In this paper, a miniaturized triple-band gap multi-via electromagnetic band gap (TBMV-EBG) structure is proposed. Lumped LC modelling method is used for the analysis of the proposed TBMV-EBG structure. Triple band gaps in both x and y-directions are obtained since TBMV-EBG unit cell consists of three resonance parallel LC circuits. Ansys (HFSS) simulation is used in eigen mode to simulate a unit cell of the proposed EBG. There is a strong agreement between simulated and experimental results. Comparing the proposed TBMV-EBG with triple band slotted EBG, triple band CSRR-EBG, fractal EBG, and dual band split EBG, size reductions of 6.52%, 7.53%, 23.21%, and 25.86% are obtained respectively which is validated by simulated and experimental results. Demonstration of the proposed TBMV-EBG structure for ultra-wideband (UWB) application is also presented. Simulation and measurement results prove that by using a single TBMV-EBG cell at the feed line of a UWB monopole antenna triple band-notches can be obtained. Moreover, switching characteristics of the proposed antenna are also demonstrated using single P-I-N diode. Depending on the ON and OFF switching status of P-I-N diode, the UWB antenna provides switching from triple band-notches to dual band-notches, respectively. The proposed switchable monopole UWB antenna as a single unit can be useful in applications wherein switching between multi-bands is desirable without changing the geometry of the structure.

1. INTRODUCTION

Band gap property of EBG structures plays an crucial role in microwave and antenna community due to their unique features. Periodicity of these EBG cells is realized by dielectric substrates metallic conductors like copper [1, 2]. Recently, many EBG structures with single/dual band gap characteristics have been reported. EBGs with triple band gaps are also required in some mobile applications like GSM900/DCS1800, global positioning system, WLAN (5.15 to 5.35 GHz, 5.725 to 5.825 GHz), and Worldwide interoperability for microwave access (WIMAX) [3, 4]. In [3], a triple band gap slotted EBG structure with four trapezoids and a co-joint small square is presented. The size of this EBG unit cell is 0.092λ at lower band gap center frequency of 1.72 GHz. In [4], a complementary split ring resonator (CSRR) is etched on conventional type of mushroom EBG to get triple bands in y-direction. The center frequencies of each band gap are 3.83 GHz, 5.67 GHz, and 9.49 GHz. The size of each EBG cell is 0.093λ at lower band gap center frequency of 3.82 GHz. In recent years, many compact dual-band EBG structures have also been reported. In [5], single EBG cell is used to get dual band-notches for UWB applications. In [6], a planar EBG design with square & circular loops is presented for radar cross section reduction (RCS) with the size of unit cell as 0.159λ at lower band gap center frequency of 3.40 GHz.

Received 23 May 2020, Accepted 29 July 2020, Scheduled 17 August 2020

* Corresponding author: Vijay R. Kapure (vijaykapure777@gmail.com).

[1] Department of Electronics Engineering, Sardar Patel Institute of Technology, Andheri (West), Mumbai-400058, India. [2] Department of Electronics and Telecommunication Engineering, Padmabhushan Vasantdada Patil Pratishthan's College of Engineering, Sion, Mumbai-400022, India. [3] Department of Electronics Engineering, Sardar Patel Institute of Technology, Andheri (West), Mumbai-400058, India.

In [7], an interdigital type of EBG [TELI-EBG] structure is introduced to reduce inband RCS of a dual-band microstrip patch antenna array. The size of each unit cell is 0.083λ at lower band gap center frequency of 5.0 GHz. In [8], a Minkowski fractal type of structure is used to design a dual-band EBG structure for GPS application with the periodic size of EBG 0.112λ at lower band gap center frequency of 1.24 GHz. Recently in [9], a split EBG with dual band gap characteristics is introduced with the unit cell of EBG 0.1160λ at lower band gap center frequency of 3.48 GHz. These presented triple/dual band gap EBG structures lacked in providing simplified structure [6] and compactness in size [3–5, 7]. As per current scenario, the antennas with triple band notches are in more demand. So in this work, a triple band EBG structure and its application for ultra-wideband (UWB) monopole antenna are demonstrated. EBG structure with triple band characteristics is achieved by introducing three parallel LC circuits per unit cell. Section 2 presents the structure, designing, and unit cell simulation of proposed triple-band multi-via electromagnetic bandgap (TBMV-EBG) in HFSS. In Section 3, the band gap measurement of TBMV-EBG is described using suspended microstrip line (SML) method. To further validate the triple band gap properties and switching functionality of proposed EBG structure, application is provided in Section 4 and Section 5. Finally, comparison study of the proposed switchable UWB monopole antenna with the reported state of art of reconfigurable antennas is concluded in Section 6.

2. PROTOTYPE OF TBMV-EBG, EQUIVALENT LC MODEL AND DISPERSION DIAGRAM

The parameters of EBG structure are explained using effective surface impedance model, with impedance of the surface assigned equal to that of a parallel resonant LC circuit, whose surface impedance (Z_s) and resonant frequency (f_c) are given as [1, 2]

$$Z_s = \frac{j\omega L}{1-\omega^2 LC} \tag{1}$$

and

$$f_c = \frac{1}{2\pi\sqrt{LC}} \tag{2}$$

where the inductance (L) and capacitance (C) are calculated as

$$L = \mu_0 h \tag{3}$$

and

$$C = \frac{w\epsilon_o(\epsilon_r+1)}{\pi}\cosh^{-1}\left\{\frac{2w+k}{k}\right\} \tag{4}$$

where (μ_0) = free space permeability, (h) = height of substrate, (w) = cell width of EBG, (k) = space separating two EBG cells, (ϵ_r) = substrate dielectric constant, and (ϵ_0) = free space permittivity.

To design a TBMV-EBG structure, three series LC resonances per unit cell are required. In order to achieve this, three vias with different slots are introduced in the proposed EBG as shown in Fig. 1. The proposed TBMV-EBG cell is designed with one outer ring, inner ring, and C-type of slot between inner and outer rings.

f_{c1}, f_{c2}, and f_{c3} of the proposed TBMV-EBG structure are given as:

$$f_{c1} = \frac{1}{2\pi\sqrt{L_1 Ceq_1}} \tag{5}$$

$$f_{c2} = \frac{1}{2\pi\sqrt{L_2 C_4}} \tag{6}$$

$$f_{c3} = \frac{1}{2\pi\sqrt{L_3 Ceq_2}} \tag{7}$$

LC model and equivalent circuit of the proposed TBMV EBG are shown in Figs. 2(a) and (b), respectively. The path between vias present on outer ring and center EBG structure represents inductance (L_1). Similarly, the path due to center EBG and joint between two inner rings introduces (L_2). (L_3) is introduced due to path between joint between two inner rings and the via of adjacent

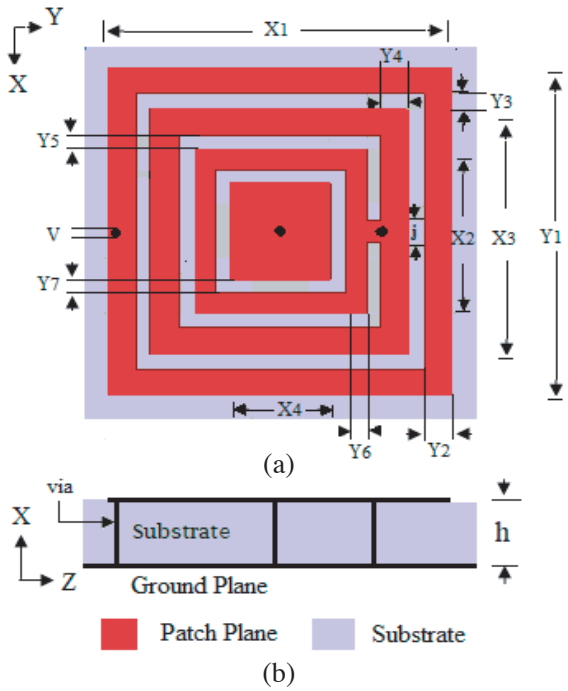

Figure 1. TBMV-EBG unit cell (a) top view (b) side view.

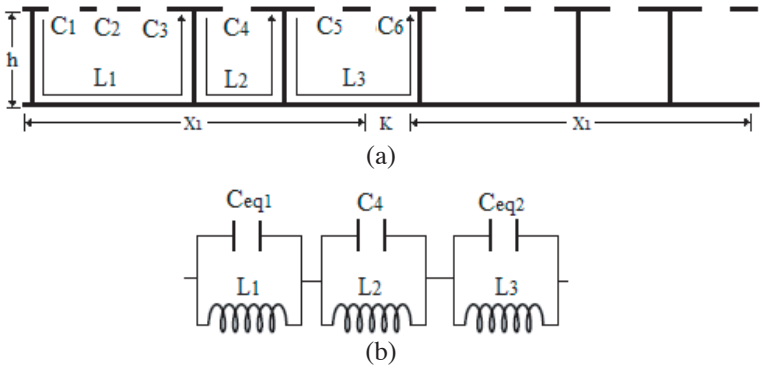

Figure 2. TBMV-EBG structure (a) LC model (b) equivalent circuit.

EBGs outer ring as shown in Fig. 1(a). Fringing effect between outer ring and inner ring (middle) gives capacitance (C_1). Similarly, middle ring and inner ring introduce (C_2). The gap between inner ring and center located square patch gives (C_3) and (C_4). Capacitance (C_5) is due to the middle ring and outer ring. The gap between two MBMV-EBG structures gives (C_6). Verification of triple band gap property of TBMV-EBG is carried out by simulation of the unit cell in eigen mode solution of Ansys HFSS [10]. The dispersion analysis of TBMV-EBG cell is carried out with rectangular symmetry (irreducible) Brillouin zone plot as shown in Fig 3. Parameters of the proposed TBMV-EBG are taken as: radius of each via (v) = 0.10 mm, dielectric constant of substrate (ϵ_r) = 2.2, $\tan\delta$ = 0.0009, height of substrate (h) = 1.57 mm, space between two EBG cells (k) = 2 mm, width of outer ring (y_2) = 1 mm, width of outer ring slot (y_3) = 0.5 mm, width of middle ring (y_4) = 1 mm, width of C-type slot (y_5) = 0.5 mm, width of inner ring (y_6) = 0.75 mm, width of inner ring slot (y_7) = 0.5 mm, (x_3) = 9 mm, (x_2) = 6 mm, width of center located square patch (x_4) = 3.5 mm, square patch width (x_1) = 12 mm, and width of joint between middle and inner rings (j) = 0.8 mm. The dispersion diagram seen in Fig. 3 clearly shows three

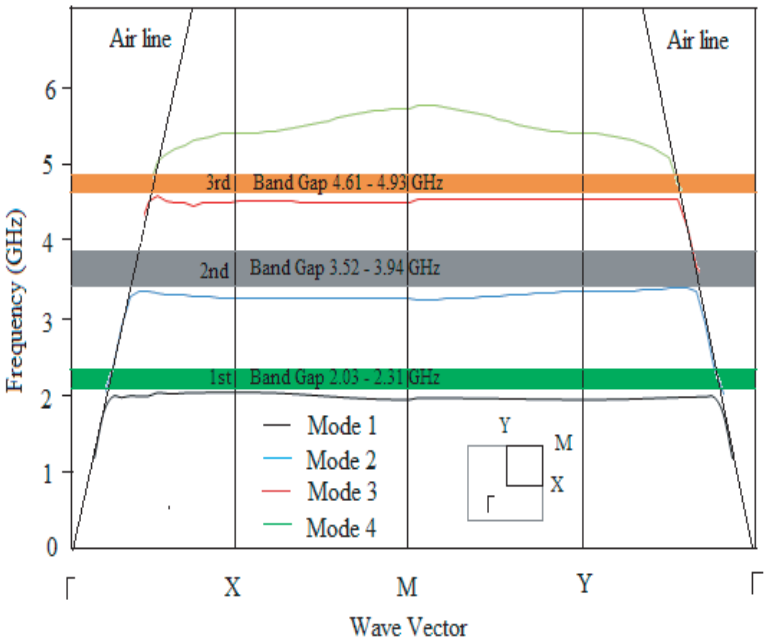

Figure 3. Dispersion diagram for TBMV-EBG structure.

bandgaps for the proposed tripleband EBG. The band gap shown in green colour (the first bandgap) is noted between mode-1 and mode-2 with lower cutoff frequency $(f_{l(1)}) = 2.03\,\text{GHz}$ and higher cutoff frequency $(f_{h(1)})$= 2.31 GHz centered at $(f_{c(1)}) = 2.17\,\text{GHz}$. The band gap in gray colour (the second bandgap) is noted between mode-2 and mode-3 centered at $(f_{c(2)}) = 3.73\,\text{GHz}$ with $(f_{l(2)}) = 3.52\,\text{GHz}$ and $(f_{h(2)}) = 3.94\,\text{GHz}$. The band gap shown in orange colour (the third bandgap) is noted between mode-3 and mode-4 centered at $(f_{c(3)}) = 4.77\,\text{GHz}$ with $(f_{l(3)}) = 4.61\,\text{GHz}$ and $(f_{h(3)}) = 4.93\,\text{GHz}$. The fractional bandwidths for three band gaps are 12.9%, 11.2%, and 6.70%, respectively. Table 1 shows the parametric observations obtained from simulation results. From the parametric study it is observed that as the values of (y_3), (y_5), and (y_7) increase, fringing effect is also increased which gives more capacitance and vice-versa. Therefore from Eq. (2), we get lower $(f_{c(1)})$, $(f_{c(2)})$, and $(f_{c(3)})$ respectively with the same period of TBMV-EBG.

Table 1. Simulated center frequencies for first, second and third band gap of TBMV-EBG with (ϵ_r) and (h) constant*.

		Center Frequencies (GHz)		
	(mm)	$(f_{c(1)})$	$(f_{c(2)})$	$(f_{c(3)})$
y_3	0.3	1.97	3.79	4.71
	0.5	2.17	3.73	4.77
	0.7	2.29	3.67	4.76
y_7	0.3	2.16	3.61	4.47
	0.5	2.17	3.73	4.77
	0.7	2.15	3.62	4.85
y_5	0.3	2.19	3.48	4.60
	0.5	2.17	3.73	4.77
	0.7	2.15	3.82	4.65

* When one parameter is varied, other parameters are kept constant.

3. MEASUREMENT OF BAND GAP OF TBMV-EBG

In this section, the validation of characteristics of TBMV-EBG structure using SML method in x- and y-directions (rectangular symmetry) is presented [11]. An array of 5×5 cells of the proposed EBG structure is printed on Rogers Diclad 880 with dielectric constant of substrate (ϵ_r) = 2.2, $\tan\delta = 0.0009$, height of substrate (h) = 1.57 mm, and other geometry parameters are kept the same as mentioned in earlier

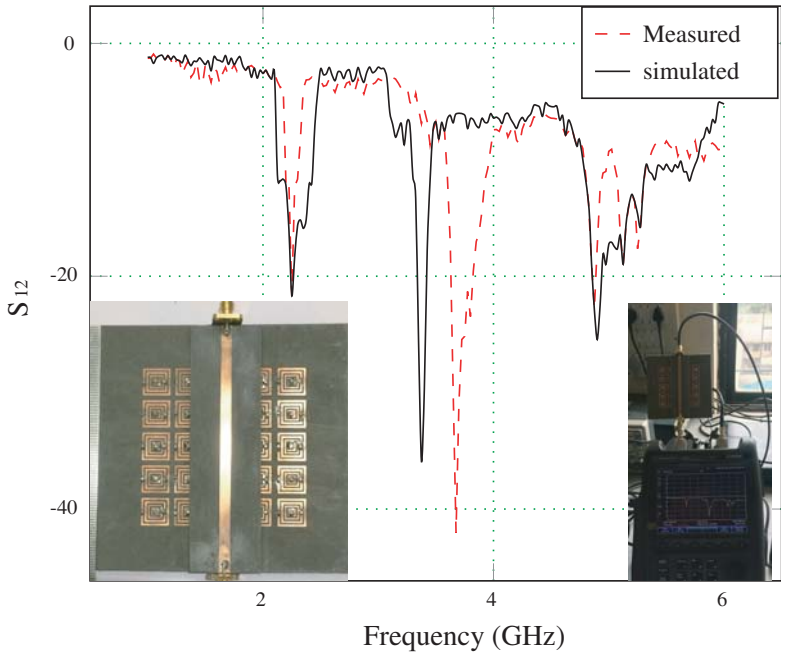

Figure 4. Experimental setup, Fabricated 5×5 array of TBMV-EBG, and measured S_{12} with SML in x-direction.

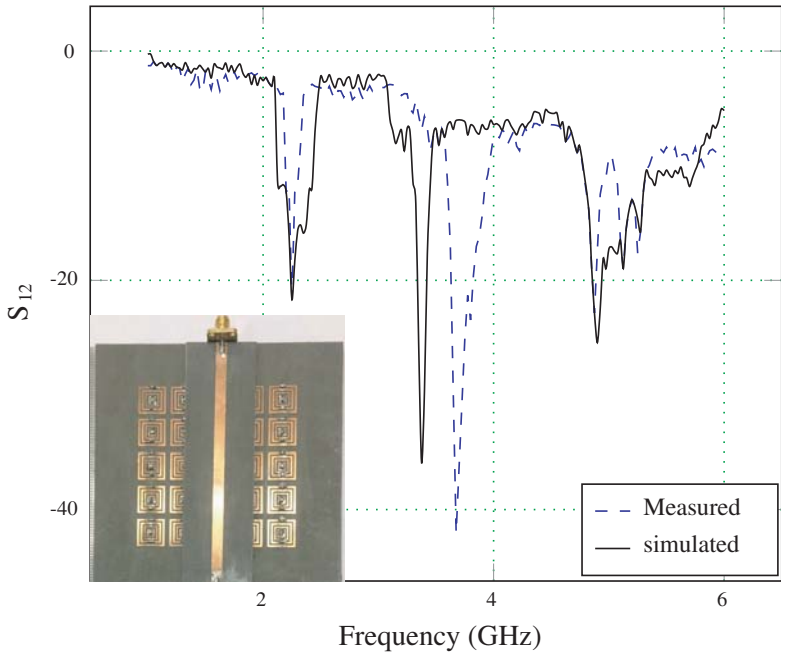

Figure 5. Fabricated 5×5 array of TBMV-EBG, and measured S_{12} with SML in y-direction.

section. The microstrip line of 50 Ω characteristic impedance and the surface of EBG are separated by 1 mm with an air gap of 0.2 mm above the EBG surface. Rogers substrate of 0.8 mm with $(\epsilon_r) = 2.2$, tan $\delta = 0.0009$ is used as supporting material. Measurement of the proposed TBMV-EBG is carried out on Agilent network analyzer with the maximum measurable frequency at 14.00 GHz as shown in Fig. 4. Fig. 4 and Fig. 5 show the fabricated structure and S_{12} measurements of TBMV-EBG using SML method in x-and y-directions, respectively. It is observed that triple band gaps are obtained with center frequencies $(f_{c(1)}) = 2.25$ GHz, $(f_{c(2)}) = 3.67$ GHz, and $(f_{c(3)}) = 4.87$ GHz both in x and y directions. The measurement results agree with simulation ones. Fabrication errors are mainly due to the difference between measurement and simulation readings, and the error at the joint of SMA connector. A tolerance margin about 5–10% should be acceptable between measurement and simulation results. Table 2, shows experimental comparison of the proposed TBMV EBG with the other reported dual/triple band EBG structures in terms of unit cell size.

4. SWITCHABLE TBMV STRUCTURE

In modern wideband communications, incorporating switching functionality for an antenna over a UWB frequency range is gaining more importance. In the UWB spectrum, there are some bands whose frequencies vary from country to country. Moreover, the antenna once designed and fabricated for fixed notch frequencies becomes difficult to be used for other applications. To overcome this issue, it is necessary to design a switchable band-notched UWB antenna for multiband applications wherein the same antenna configuration can be used for multiple systems. Switching to the desired frequency bands of antenna can be done with the help of active elements such as P-I-N diodes and switches. Based on the ON and OFF status of diodes, the same UWB antenna can be swapped to desired working frequency bands. In this section, a P-I-N diode SMP 1352 is inserted in the proposed TBMV EBG structure [12]. The configuration of TBMV EBG with P-I-N- diode is shown in Fig. 6. The modelling of the P-I-N diode can be realised as an RLC circuit consisting of low resistance permitting current to pass through the diode and act as a short circuit in the ON state, while in the OFF state it acts as an open circuit.

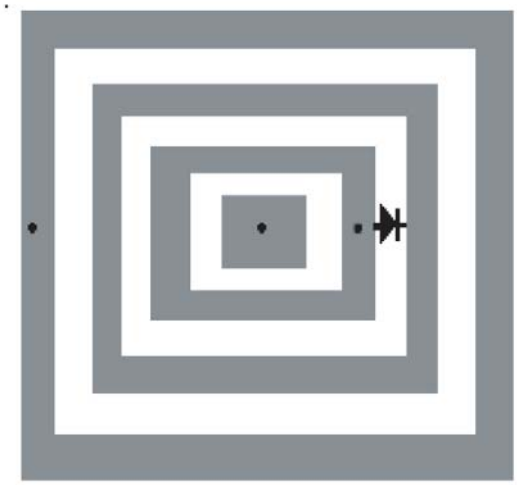

Figure 6. TBMV-EBG cell with switchable P-I-N diode.

5. SWITCHABLE DUAL/TRIPLE UWB BAND NOTCHED ANTENNA USING P-I-N DIODE

Besides having fast switching time and low cost, easy integration of active devices with UWB antennas has certainly paved a path for achieving reconfiguration using a single antenna device. Previously, many techniques were proposed to provide band-notching. In [13–20], these band notches are achieved by etching slots on radiating elements, using resonators, or with multi-parasitic elements. However

Table 2. Experimental comparison of proposed TBMV-EBG with other EBGs.

Ref.	ϵ_r/h (mm)	No. of Layers	$f_{c(1)}/f_{c(2)}/f_{c(3)}$ (GHz)	Patch width
[3]	3.2/0.76	single	1.72/4.74/7.04	$0.092\lambda_{c(1)}$
[4]	2.2/2.00	single	3.83/5.67/9.49	$0.093\lambda_{c(1)}$
[6]	2.2/6.35	single	3.40/9.40/N.A.	$0.159\lambda_{c(1)}$
[7]	2.65/2.00	double	5.00/7.50/N.A.	$0.083\lambda_{c(1)}$
[8]	4.0/1.52	single	1.24/1.78/N.A.	$0.112\lambda_{c(1)}$
[9]	4.4/1.2	single	3.48/4.86/N.A.	$0.1160\lambda_{c(1)}$
P. E.	**2.2/1.57**	**single**	**2.17/3.73/4.77**	$0.086\lambda_{c(1)}$

N.A. = Not Applicable, P. E. = Proposed EBG.

the technique of inferring the antenna to get notch bands affects the performance of antenna. Due to space restriction and coupling between multi-parasitic elements, it is difficult to achieve multi-notch characteristics for UWB monopole antenna with minimum cells. The work presented in this article overcomes this issue by placing a single unit cell of TBMV-EBG near the feedline of a UWB monopole antenna. Also, frequency reconfigurations of antennas are obtained by using active devices such as capacitors, switches, or diodes incorporated within these designs. By controlling the states or changing the capacitance of these active devices, switching or tuning between different operating bands is achieved. In [13], reconfiguration characteristics of an antenna are obtained by using three switches in L-shaped and U-shaped slots, respectively. Single or dual notched bands at 5.5 GHz and 3.5 GHz are obtained by controlling the states of switches. The frequency reconfiguration in [14] is achieved by inserting two switches/P-I-N diodes in the two DSRR (double split ring resonator) structure. Depending on the on/off status of switches/P-I-N diodes, the antenna is switched between dual band-notches and no band-notch in the UWB range, respectively. [15] reports a tunable band notched UWB Heart-Shaped Planar Monopole Antenna with an annular slot. The single notch band is reconfigured by inserting a varactor in the annular slot and tuning the antenna in range extending from 4.62 to 5.83 GHz. In [16], a reconfigurable filtering antenna is presented, wherein dual band rejections are obtained at 2.4 GHz and 5.8 GHz by using an open loop filter and a hairpin filter, respectively. The reconfiguration in this structure is achieved by three P-I-N diodes. In [17], a switchable planar monopole antenna is designed with two capacitors inserted within the the resonators. By changing the capacitance values, the antenna is switched between UWB and narrow bands. A band-notched antenna reconfigured between 3 and 4 GHz (WIMAX) with fixed (WLAN) notched band is presented in [18]. This is done by continuously tuning two variable capacitors embedded in the structure. In [19], a switchable dual band notch antenna is fabricated and tuned to produce dual band notches using four capacitors within the resonators. In [20], a UWB antenna with two EBG structures namely TVEL and fractal is used to obtain dual band notches at WLAN and WIMAX bands, respectively. Frequencies are tuned between 2.8–4.0 GHz and 4.7–6.2 GHz by integrating two varactor diodes into EBGs independently. The work presented in [13–20] have managed to achieve reconfigurability with more active devices. As more active devices increase the power supply requirement, it is always desirable to have fewer active devices thereby minimizing complexity in design. So the approach is to design a UWB monopole antenna which would produce multiple band notches and can be switched from triple band notches to dual band notches using only one active device, i.e., P-I-N diode embedded within the TBMV-EBG unit cell. Table 3 shows the comparison of different reconfigurable band-notched antennas with the proposed antenna. From the comparison it is observed that the proposed switchable dual/triple band antenna proves to be a strong candidate wherein the switching between dual/triple notches using a single structure is desirable.

5.1. Fork Type UWB Monopole Antenna

Reference fork type monopole antenna is shown in Fig. 7(a) with $(\epsilon_r) = 2.2$, $\tan\delta = 0.0009$, and $h = 1$ mm. The fork type of monopole antenna as shown in Fig. 7(a) is used as the reference antenna for

further design. The antenna is etched with a size of $35 \times 35\,\text{mm}^2$ on a substrate with height 1 mm. The ground plane of the reference antenna is etched by quasi semi-circular slot. The microstrip feed width is kept as 1.5 mm, and the other parameters of proposed antenna are: $(L_1) = 35\,\text{mm}$, $(W_1) = 35\,\text{mm}$, $(L_2) = 12\,\text{mm}$, $(L_3) = 13.6\,\text{mm}$, $(L_4) = 2.1\,\text{mm}$, $(L_5) = 9\,\text{mm}$, $(L_6) = 1.6\,\text{mm}$, $(W_2) = 6\,\text{mm}$, $(W_3) = (W_4) = 2.1\,\text{mm}$, $(W_5) = 1.8\,\text{mm}$. Simulated VSWR of the fork-type reference antenna is shown in Fig. 8. A fairly good matching of impedance is observed with VSWR < 2 without any band notches for ultrawideband range (3.1–10.6) GHz.

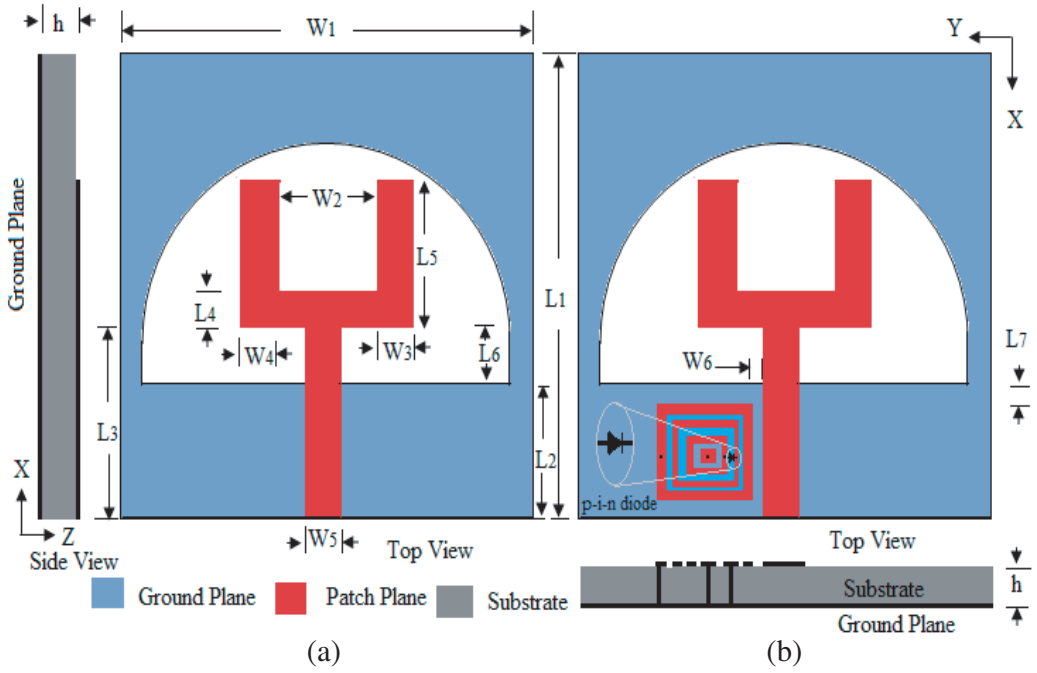

Figure 7. Configuration of fork-type monopole antenna (a) without TBMV-EBG, and (b) with TBMV-EBG and P-I-N diode.

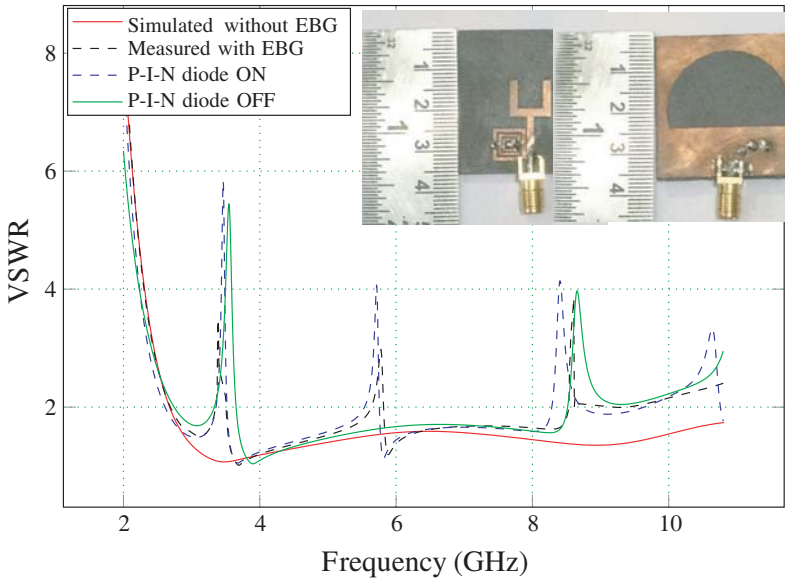

Figure 8. Photograph, simulated and measured VSWR of fork-type monopole antenna with TBMV-EBG and P-I-N diode ON and OFF conditions.

Table 3. Comparison of TBMV-EBG and other EBG structures used for getting band-notch and reconfiguration in UWB monopole antennas.

Ref.	Band-Notch Technique Used	Reconfig. Done With	Active Devices Used	Tuning/ Switching Freq (GHz)
[13]	Slot	Switch	03	3.5/5.5
[14]	DSRR	P-I-N diode	02	3.4, 5.3/5.57, 3.52
[15]	Slot	varactor diode	01	4.62-5.83
[16]	BPF	P-I-N diode	03	2.4/5.8/UWB
[17]	Resonator	Capacitor	02	5.0–6.0/UWB
[18]	Resonator	Capacitor	02	3.0–4.0
[19]	Resonator	Capacitor	02	2.9–3.1/5.8–7.0
[20]	EBG	Varactor	02	2.8–4.0/4.7–6.2
P. W.	**EBG**	**P-I-N diode**	**01**	**3.39, 5.78, 8.60/3.39, 8.60**

DSRR = Double Split Ring Resonator, BPF = Band pass filter, EBG = Electromagnetic bandgap structure, P. W. = proposed work.

5.2. Fork Type UWB Monopole Antenna with TBMV EBG and P-I-N Diode

A UWB fork-type antenna with a single TBMV EBG cell and P-I-N diode is shown in Fig. 7(b). The EBG cell is placed near the feed line of UWB monopole antenna, and simulation is done using Ansys HFSS. Parameters of the reference antenna are similar to those mentioned in the previous section. Optimized parameters of TBMV EBG cell are: radius of each via (v) = 0.1 mm, substrate dielectric constant (ϵ_r) = 2.2, substrate height (h) = 0.8 mm, width of outer ring (y_2) = 1 mm, width of outer ring slot (y_3) = 0.4 mm, width of middle ring (y_4) = 0.7 mm, width of C-type slot (y_5) = 0.3 mm, width of inner ring (y_6) = 0.5 mm, width of inner ring slot (y_7) = 0.2 mm, (x_2) = 3.2 mm, (x_3) = 5.2 mm, center square patch width (x_4) = 1.8 mm, and square patch width (x_1) = 8 mm. The gap between the feedline and EBG cell is kept as (W_6) = 0.2 mm, and the distance between EBG cell and upper edge of quasi semi-circular slot is (L_7) = 1.2 mm. Due to the change in substrate height in this application, EBG with different sizes is considered. The simulated VSWR of UWB monopole antenna with TBMV EBG for P-I-N diode ON and OFF conditions is shown in Fig. 8. It is observed that there is no band notch for UWB monopole antenna without TBMV EBG, whereas with TBMV EBG cell, UWB antenna produces triple band notch frequencies observed at 3.46 GHz, 5.71 GHz, and 8.40 GHz (VSWR > 2 GHz) which proves that TBMV EBG exhibits triple band notch characteristics. The first notch bandwidth of 0.24 GHz is obtained between 3.34 GHz and 3.58 GHz with the notch frequency of 3.46 GHz. The second notch bandwidth of 0.52 GHz is obtained between 5.44 GHz and 5.96 GHz with the notch frequency of 5.71 GHz. The third notch bandwidth of 0.19 GHz is obtained between 8.31 GHz and 8.50 GHz with the notch frequency of 8.40 GHz. The measured VSWR of UWB fork-type antenna with TBMV-EBG is plotted in Figure 8. From the graph it is observed that the simulated and measured results are in good agreement. The antenna exhibits high impedance mismatching at the first notch producing high VSWR as compared to subsequent notches obtained at higher frequencies.

During the ON state of P-I-N diode, three notch frequencies are observed whereas during OFF state two notch frequencies are observed. Simulated real and imaginary parts of impedance of the reference antenna without TBMV EBG are shown in Figs. 9(a) and (b), respectively. Similarly, simulated real and imaginary parts of impedance of the reference antenna with TBMV EBG for P-I-N diode ON and OFF conditions are shown in Figs. 9(a) and (b), respectively. Real and imaginary parts of the impedance go away from 50 Ω and 0 Ω line respectively for all notch frequencies. Fig. 10(a) shows the effect of the width of outer ring on the center frequency of the band-notch of antenna. By varying the outer ring width (y_2), a noticeable change in the third notch frequency is observed without any change in

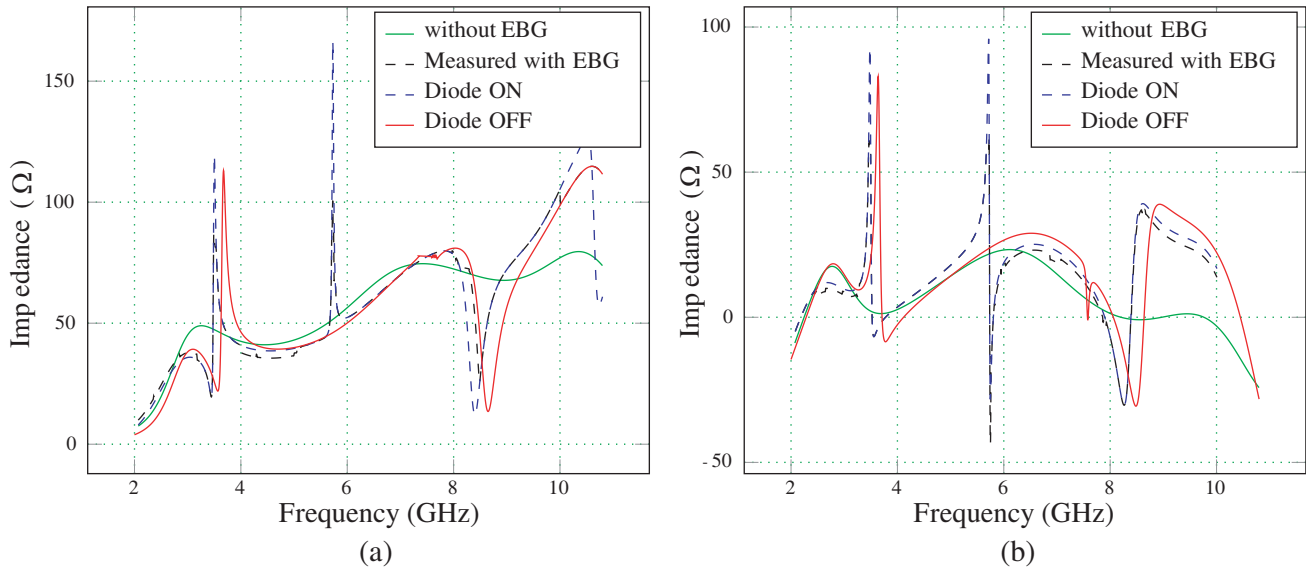

Figure 9. Simulated and measured impedance of fork type monopole antenna without TBMV-EBG, with TBMV-EBG and P-I-N diode ON and OFF (a) Real part, and (b) Imaginary part.

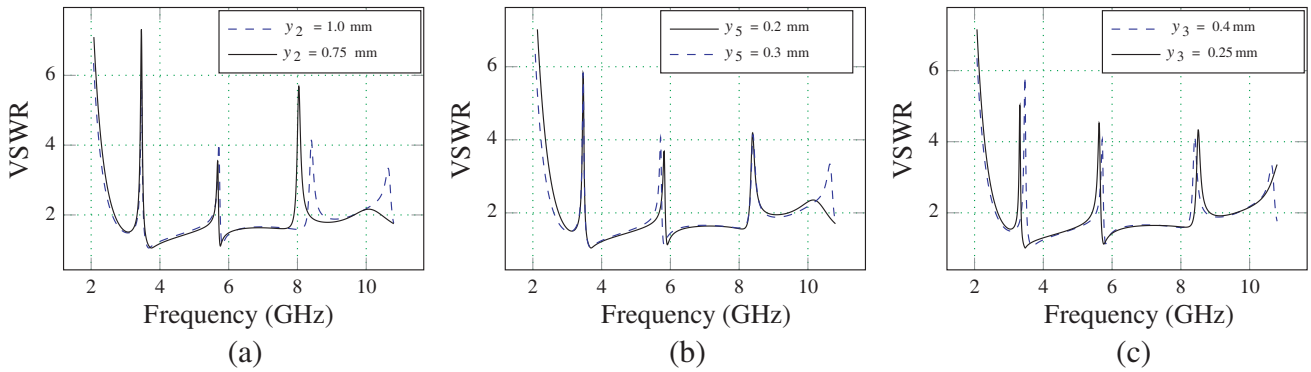

Figure 10. (a) Effect of the gap between EBG cell and feedline, and (b) Effect of the distance between EBG cell and upper edge of quasi semi-circular slot on the center frequency of the band-notch.

the first and second notches. Fig. 10(b) shows the effect of the gap between middle ring and inner ring (y_5) on the center frequency of the band-notch. Variation in (y_5) produces changes in the second notch frequency only with negligible effect on the first and third notches. The effect of the gap between outer ring and middle ring (y_3) on the center frequency of the band-notch is shown in figure 10(c). Changing (y_3) shows observable change in the first notch frequency without any significant changes in remaining two notch frequencies. It is observed that without changing the EBG periodic size, all the notch band center frequencies can be varied.

The effect of gap between EBG cell and feedline (w_6), and the distance between EBG cell and upper edge of quasi semi-circular slot (L_7) are shown in Figs. 11(a) and (b), respectively. From Fig. 11(a), it is observed that as EBG moves away from feedline, the band-notched antenna behaves as a reference UWB monopole antenna without any notches. Also variation in distance between EBG cell and upper edge of quasi semi-circular slot, as shown in Fig. 11(b), has no significant impact on the band-notched center frequencies. The maximum gain of UWB monopole antenna with TBMV EBG for P-I-N diode ON and OFF states is shown in Fig. 12. When the diode is ON, the reduction in gain is observed at the triple band notch frequencies with a good performance for other frequencies. On the contrary, when the diode is OFF, the reduction in gain is observed at the dual band notch frequencies with a good

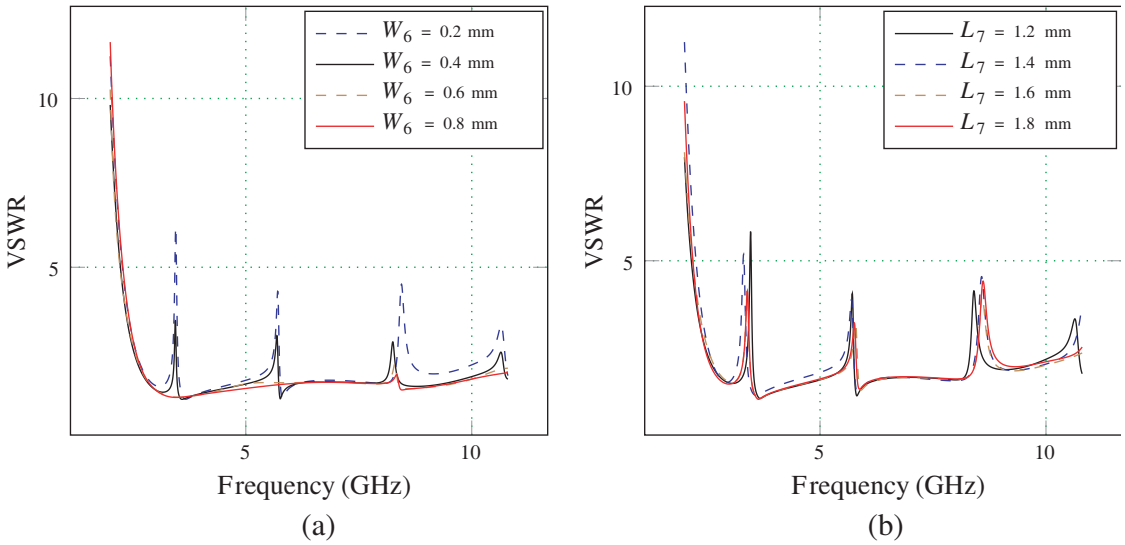

Figure 11. (a) Effect of the gap between EBG cell and feedline, and (b) Effect of the distance between EBG cell and upper edge of quasi semi-circular slot on the center frequency of the band-notch.

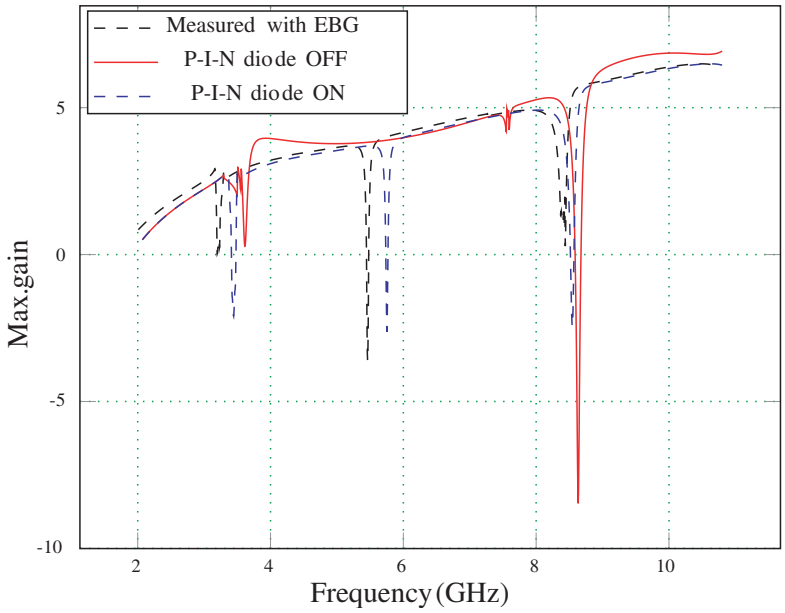

Figure 12. Simulated and measured gain of fork-type UWB monopole antenna with TBMV-EBG and P-I-N diode ON and OFF conditions.

performance for other frequencies as shown in Fig. 12. Measured radiation patterns of reference antenna with TBMV-EBG are shown in Fig. 13. The antenna shows good bidirectional pattern in E-plane and omnidirectional pattern in H-plane at 4.00 GHz, but at higher frequency of 8.00 GHz these patterns are slightly degraded due to the presence of undesired higher order resonance modes. Similarly, radiation patterns of reference antenna without TBMV EBG and with TBMV EBG, and P-I-N diode in E-(electric field) plane and H-(magnetic field) plane at 4.00 GHz and 8.00 GHz are shown in Fig. 14. The antenna shows a similar bidirectional pattern in E-plane (x-y) and omnidirectional pattern in H-plane (y-z) with and without TBMV EBG.

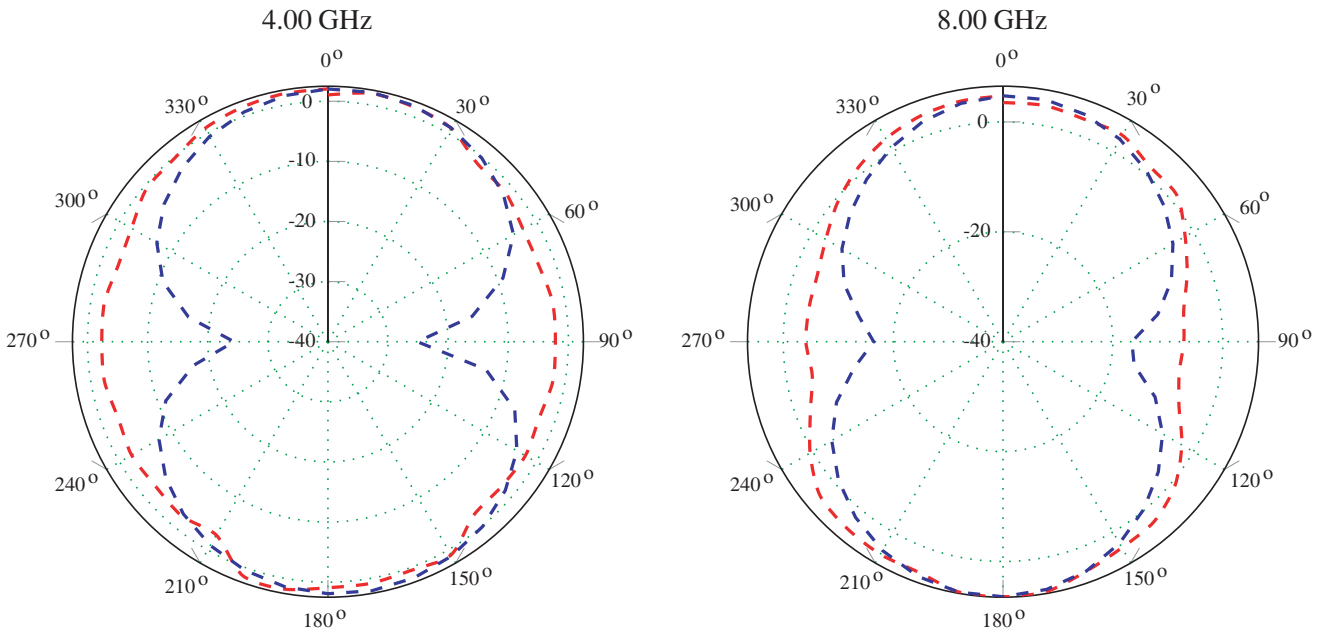

Figure 13. Measured radiation pattern for E-plane (x-z), and H-plane (y-z) of fork-type monopole antenna with TBMV-EBG (--- E-plane, and --- H-plane).

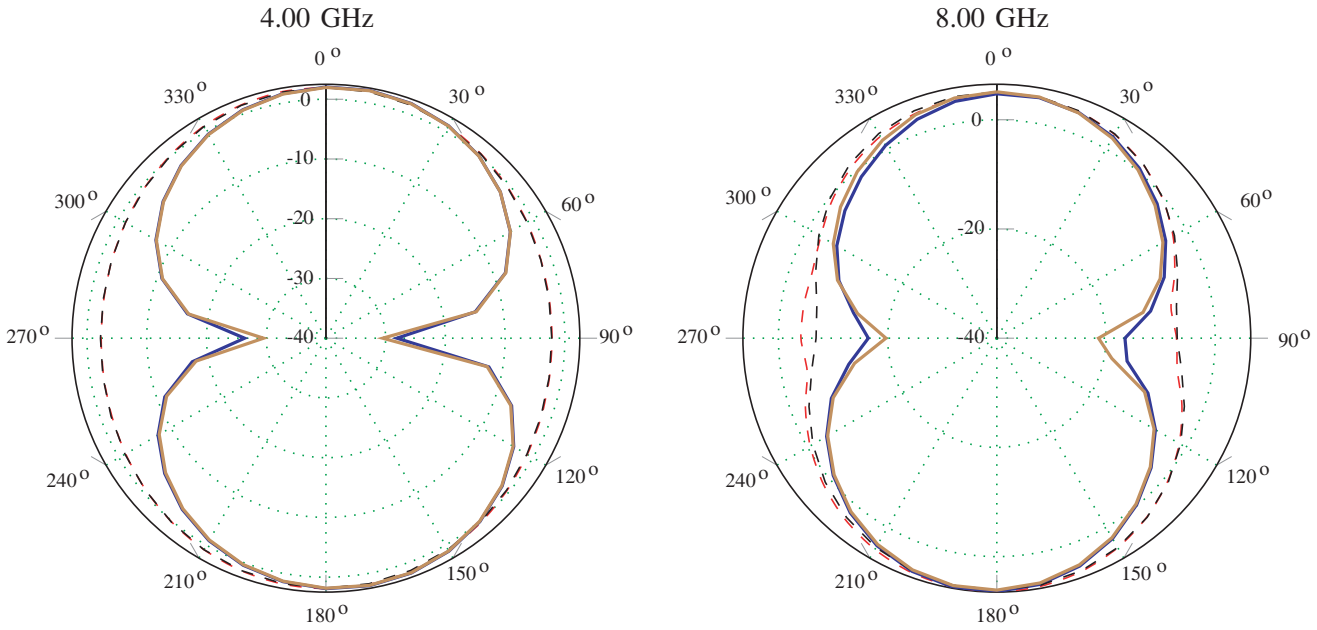

Figure 14. Radiation pattern for E-plane (x-z), and H-plane (y-z) of fork-type monopole antenna without TBMV-EBG, and with TBMV-EBG and P-I-N diode (—— E-plane, --- H-plane with EBG, and —— E-plane, --- H-plane without EBG).

6. CONCLUSION

In this paper, a miniaturized triple-band gap multi-via electromagnetic band gap (TBMV-EBG) structure has been presented. The analysis, simulation, and results of the proposed EBG are also validated experimentally. Triple band gaps in both x- and y-directions are obtained since TBMV-EBG unit cell consists of three resonance parallel LC circuits. The periodic size of TBMV-EBG is only 0.086λ at the expected lower band gap center frequency. Comparing proposed TBMV-EBG with triple band slotted EBG, triple band CSRR-EBG, fractal EBG, and dual band split EBG, size reductions of 6.52%, 7.53%, 23.21%, and 25.86% are obtained, respectively. Simulated and measured results prove that by using a single TBMV-EBG cell at the feed line of a UWB monopole antenna, triple band-notches can be obtained. Moreover, switching characteristics of the proposed antenna are also demonstrated using single P-I-N diode. Depending on the ON and OFF switching status of P-I-N diode, the UWB antenna provides switching from triple band-notches to dual band-notches, respectively. The proposed switchable monopole antenna as a single unit can be useful in applications wherein switching between multi-bands is desirable without changing the geometry of the structure.

REFERENCES

1. Sievenpiper, D., L. Zhang, Romulo, J. Broas, N. Alexopolous, and E. Yablonovith, "High impedance electromagnetic surfaces with a forbidden frequency band," *IEEE Trans. Microw. Theory Tech.*, Vol. 47, No. 11, 2059–2074, Nov. 1999.
2. Yang, F. and Y. Rahmat-Samii,"Microstrip antennas integrated with electromagnetic band-gap (EBG) structures: A low mutual coupling design for array applications," *IEEE Trans. Antennas Propag.*, Vol. 51, No. 10, 2936–2946, Oct. 2003.
3. Xie, H.-H., Y.-C. Jiao, K. Song, and Z. Zhang "A novel multi-band electromagnetic bandgap structure," *Progress In Electromagnetics Research Letters*, Vol. 9, 67–74, 2009.
4. Peng, L., C. Ruan, and Z. Li, "A novel compact and polarization-dependent mushroom-type EBG using CSRR for dual/triple-band applications," *IEEE Microw. Wireless Compon. Lett.*, Vol. 20, No. 09, 489–491, Sept. 2010.
5. Bhavarthe, P. P., S. S. Rathod, and K. T. V. Reddy,"Compact dual band gap electromagnetic bandgap structure," *IEEE Trans. Antennas Propag.*, Vol. 67, No. 1, 596–600, Jan. 2019.
6. Chen, W., C. Balanis, and C. Birtcher,"Dual wide-band checkerboard surfaces for radar cross section reduction," *IEEE Trans. Antennas Propag.*, Vol. 64, No. 9, 4133–4138, Sept. 2016.
7. Zhang, S., "Novel dual-band compact HIS and its application of reducing array in-band RCS," *Microwave and Optical Technology Letters*, Vol. 58, No. 3, 700–704, Mar. 2016.
8. Bao, X. L., G. Ruvio, and M. J. Ammann, "Low-profile dual-frequency GPS patch antenna enhanced with dual-band EBG structure," *Microwave and Optical Technology Letters*, Vol. 49, No. 11, 2630–2634, Nov. 2007.
9. Tan, X., W. Wang, Y. Wu, Y. Liu, and A. Kishk, "Enhancing isolation in dual-band meander-line multiple antenna by employing split EBG structure," *IEEE Trans. Antennas Propag. (Early access)*, Vol. 67, No. 4, Apr. 2019.
10. Remski, R., "Analysis of photonic bandgap surfaces using ansoft HFSS," *Microwave Journal*, Vol. 43, No. 9, 190–199, Sept. 2000.
11. Yang, L., M. Fan, F. Chen, J. She, and Z. Feng, "A novel compact electromagnetic-bandgap (EBG) structure and its application for microwave circuits," *IEEE Trans. Microw. Theory Tech.*, Vol. 53, No. 1, 183–190, Jan. 2005.
12. Skyworks, "SMP1352 series: Large signal switching, plastic packaged PIN diodes," *Datasheet*, Jun. 2012.
13. Gao, G., B. Hu, L. He, S. Wang, and C. Yang, "Investigation of a reconfigurable dual notched UWB antenna by conceptual circuit model and time domain characteristics," *Microwave and Optical Technology Letters*, Vol. 59, 1326–1332, Jun. 2017.

14. Alhegazi, A., Z. Zakaria, N. A. Shairi, I. M. Ibrahim, and S. Ahmed, "A novel reconfigurable UWB filtering-antenna with dual sharp band notches using double split ring resonators," *Progress In Electromagnetics Research C*, Vol. 59, 185–198, Nov. 2017.
15. Hua, C., Y. Lu, and T. Liu, "UWB heart-shaped planar monopole antenna with a reconfigurable notched band," *Progress In Electromagnetics Research Letters*, Vol. 65, 123–130, Jan. 2017.
16. Deng, T., S. Hou, L. Zhao, and L. Guo, "A reconfigurable filtering antenna with integrated bandpass filters for UWB/WLAN applications," *IEEE Trans. Antennas Propag.*, Vol. 66, No. 1, 401–404, Jan. 2018.
17. Nejatijahromi, M., M. Naghshvarianjahromi, and M. Rahman, "Switchable planar monopole antenna between ultra-wideband and narrow band behavior," *Progress In Electromagnetics Research Letters*, Vol. 75, 131–137, May 2018.
18. Nejatijahromi, M., M. U. Rahman, and M. Naghshvarianjahromi, "Continuously tunable WiMAX band-notched UWB antenna with fixed WLAN notched band," *Progress In Electromagnetics Research Letters*, Vol. 75, 97–103, May 2018.
19. Nejatijahromi, M., M. Naghshvarianjahromi, and M. Rahman, "Compact CPW fed switchable UWB antenna as an antenna filter at narrow-frequency bands," *Progress In Electromagnetics Research C*, Vol. 81, 199–209, Feb. 2018.
20. Trimukhe, M. A. and B. G. Hogade, "Compact UWB antenna with tunable band-notch characteristics using varactor diode," *Progress In Electromagnetics Research C*, Vol. 97, 15–28, Nov. 2019.